

Drag and dynamic maneuvering forces on a submersible

Both manned and unmanned underwater vehicles are widely used for research, equipment installation and maintenance, and as weapons. The increased sophistication and changes in operational environment of these systems have put a new emphasis on all aspects of design including hydrodynamic performance. The problem of designing submarine vehicles for low drag and good handling and stability has been the subject of many studies dating back to the beginning of the last century. These vehicles need to be both maneuverable and easy to control. Traditionally submersibles have been designed with extensive model testing in which the hydrodynamic forces are determined in a series of static experiments. These forces are then characterized by hydrodynamic coefficients and which are then used in relatively simple computer simulation in which the forces assumed to be functions of the coefficients and parameters such as speed, angle of attack, etc. The nonlinear nature of the means that the coefficients are not constant over a wide range of attitudes and speeds so many experiments are required for the initial characterization. This approach is time consuming and ignores the added mass effects due to acceleration.

In a recent study (Reference 1) AcuSolve™ was used to calculate the forces on a standardized submarine hull shape (DARPA SUBOFF) over an extensive range of conditions. Two hull configurations were tested, a bare hull as shown in and a hull with sail and appendages as shown in Figure 1. The predicted force resultants and flow details were compared with laboratory experiments for static configurations (constant attitude and speed). In addition, dynamic simulations were used to demonstrate the importance of added mass effects.

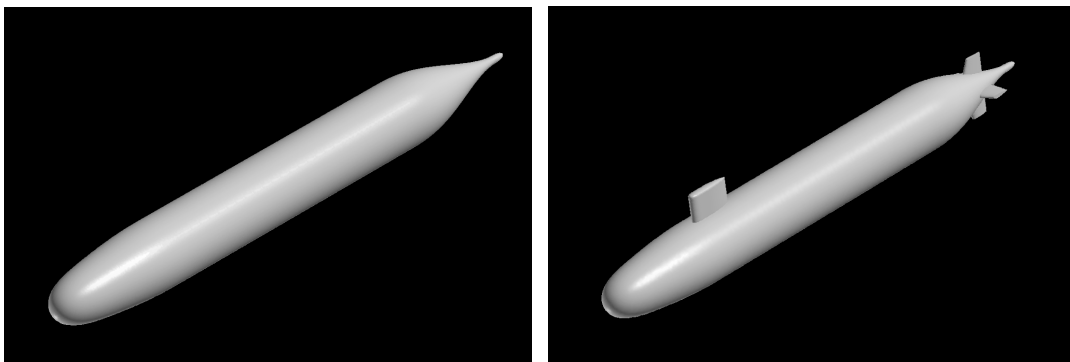


Figure 1. Hull geometries

Because the end objective is to use AcuSolve to predict the dynamics response of the submersible including dynamic effects such as eddies and added mass effects all of the simulations were completed using Spalart's Delayed Detached Eddy Simulation (DDES) model.

In addition, AcuSolve's wall function implementation is used to reduce problem size and all meshes were generated using AcuConsole for reduced problem turnaround time. Problem size was 2.08M nodes for the bare hull geometry and 2.25M nodes for the full SUBOFF geometry. Both meshes used AcuSolve's fluid-fluid interface with a cylindrical inner mesh so that pitch can be changed dynamically without distorting the mesh.

The comparisons with experiments examined both the overall forces on the model which are used to determine the maneuvering coefficients and also the surface pressures and skin friction as well as the flow field around the model under static conditions. Figures 2 and 3 compare the surface pressure and skin friction predicted by AcuSolve with measurements made in the model experiments at a Reynolds number of 14 million.

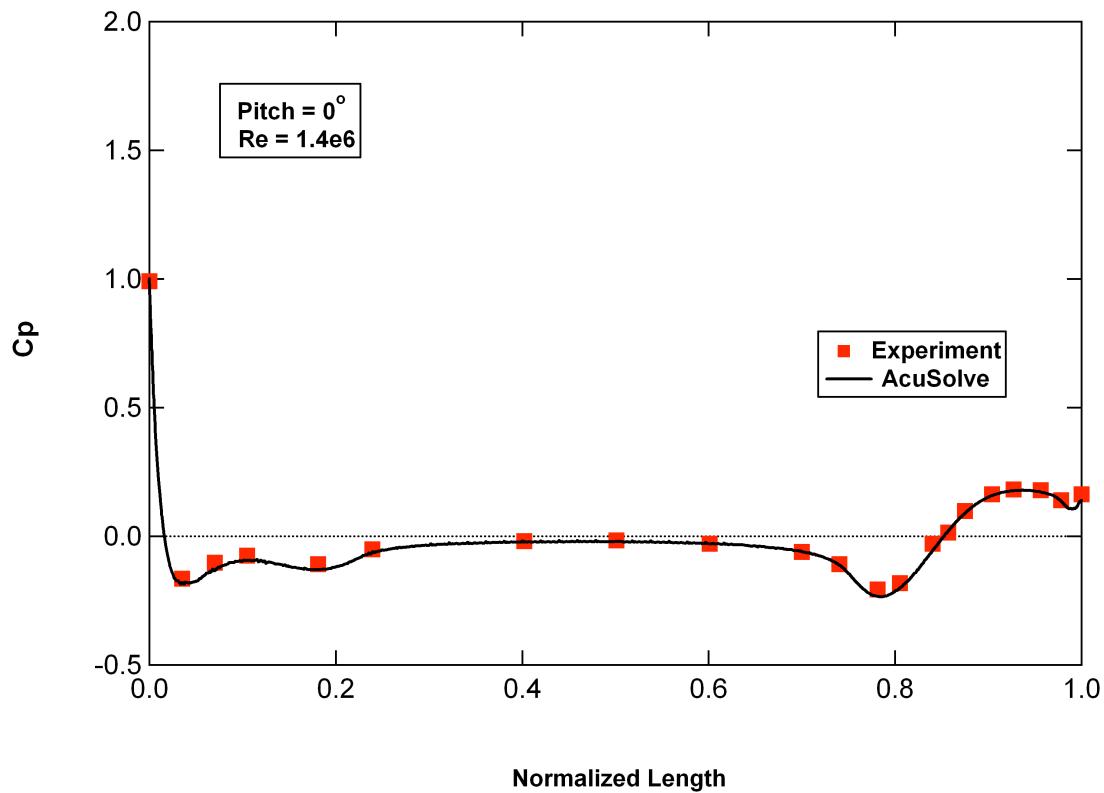


Figure 2. Comparison of predicted and measured surface pressure on bare hull

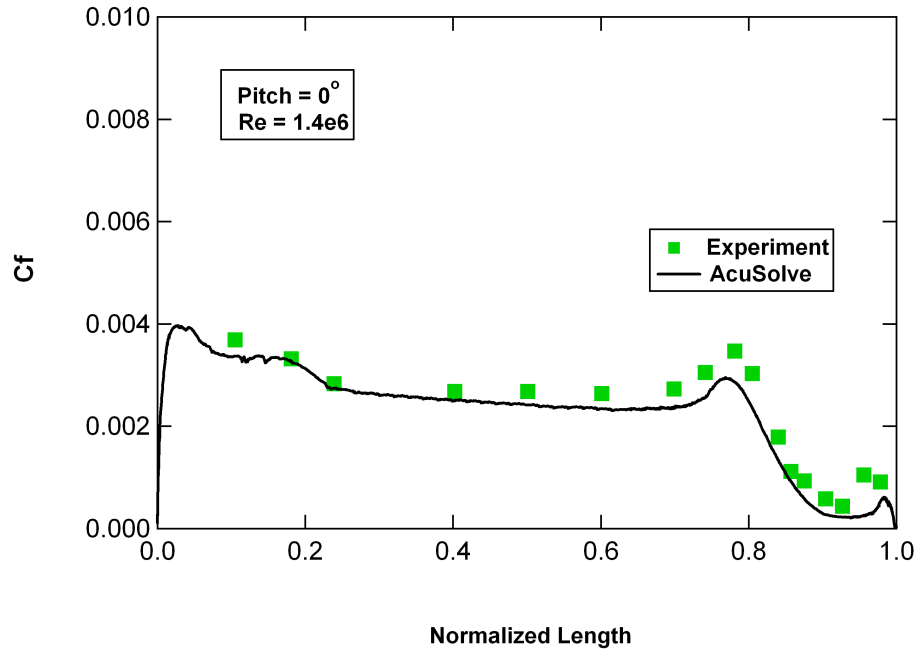


Figure 3. Comparison of predicted and measured skin friction on bare hull

The SUBOFF experimental data includes extensive measurements of the resultant forces for a wide range of angles of attack. These are well predicted in the AcuSolve simulations. For example Figure 4 shows the axial force (thrust) and vertical force (lift) on the bare hull as a function of pitch angle as measured in the experiments and predicted by AcuSolve.

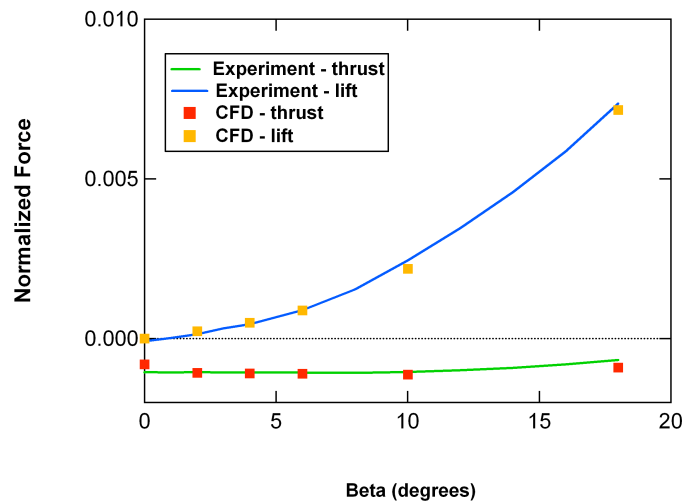


Figure 4. Resultant forces on bare hull as a function of pitch angle

Finally, dynamic calculations were used to demonstrate the importance of added mass and eddies in determining submersible response. In one simulation, the full SUBOFF is forced to undergo a simple diving maneuver in which the submersible smoothly pitches from 0 degrees (level) to 10 degrees downward and returns to 0 degrees. Figure 5 shows a visualization of the axial component of vorticity on several planes along the hull during the maneuver. This is a visualization of the vortex structures around the hull.

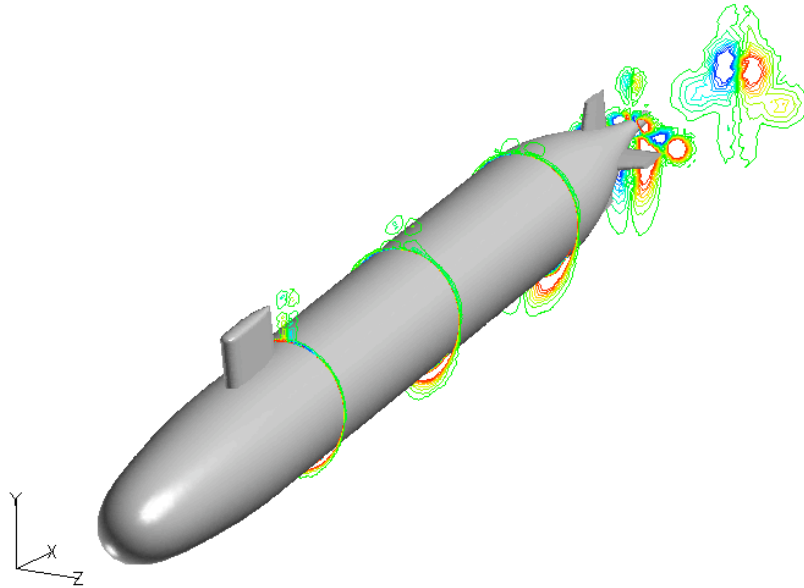


Figure 5. X-vorticity components around hull during diving maneuver

Figure 6 plots the pitching moment on the hull and compares it to a simple analysis based on the static data described earlier. This shows significant differences between the static and dynamics calculations.

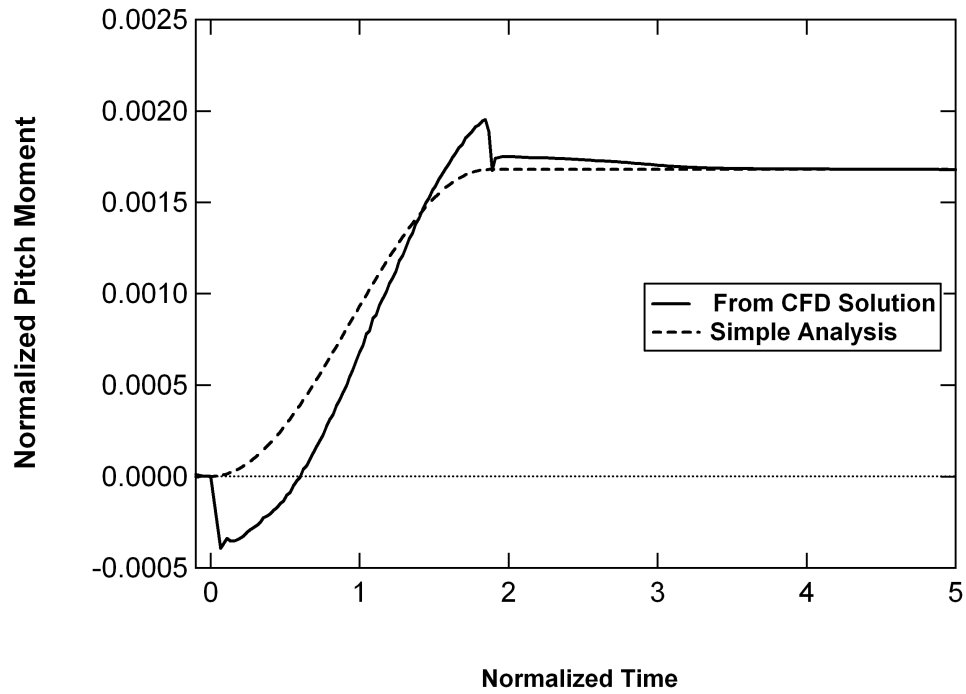


Figure 6. Pitching moment for dynamic calculations contrasted with that predicted by static hydrodynamic coefficients